The WSe_2/Tungsten-Oxide Interface: Structure and Photoluminescence

R. Tenne, K. Eherman, and D. Mahalu

Department of Materials and Interfaces, Weizmann Institute, Rehovot 76100, Israel

M. Peisach

National Accelerator Laboratory, Faure 7212, South Africa

W. Kautek

Laboratory for Chemical Surface Technologies, Federal Institute for Materials Research and Testing, Unter den Eichen 87, D-1000 Berlin 33, Germany

A. Wold

Department of Chemistry, Brown University, Providence, Rhode Island 02912, USA

R. Matson

National Renewable Energy Laboratory, 1617 Cole Blvd., Golden 80401-3393, Colorado, USA

D. H. Waldeck

Department of Chemistry, University of Pittsburgh, Pittsburgh, Pennsylvania 15260, USA

Key Words: Luminescence / Photoelectrochemistry / Semiconductors / Surfaces

A "mixed" surface of WSe_2, which contains both the $||c$ and $\perp c$ facets was produced by mechanical indentation, followed by photoelectrochemical etching, and chemical cleaning. This surface was shown to exhibit low surface recombination velocity, and consequently high solar to electrical conversion efficiency, in the past. Using O^{18} as a tracer for nuclear activation analysis it is shown that, after the above surface treatment, the surface of the $||c$ facet is covered with a thin (3 – 5 monolayers) film of tungsten oxide. The structure of the crystalline oxide phases that comprise the tungsten-oxide/WSe_2 interface are investigated with powder X-ray diffraction. X-ray photoelectron spectroscopy is used to study the chemical bonding at the interface. A model is proposed to explain the absence of surface recombination at this interface.

A strong above the bandgap luminescence is observed from $||c$ facets of "mixed" surfaces, and from crystal edges ($||c$) which were allowed to "age" for a few weeks in the air. The origin of this luminescence was investigated in some detail, and a mechanism, involving partially oxidized $||c$ surface which possibly leads to quantum confinement of excitons in $||c$ edges of WSe_2, is proposed.

1. Introduction

Layered transition dichalcogenide semiconductors are promising materials for solar energy conversion. They have optical absorption in the visible and infra-red (IR) parts of the spectrum, which ensures high absorption of the solar irradiation [1 – 3]. In addition to that they can be doped both n- and p-type [4]. The most intriguing property of these materials, however, was proposed by Tributsch [5], who concluded that the fundamental photoexcitation process of valence band electrons involves d-d transitions that do not lead to the cleavage of the chemical bond, at the surface. Consequently these materials are stable against photocorrosion in polyiodide solutions, which is prevalent in many semiconductors, making them unsuitable for photovoltaic applications. Respectable conversion efficiencies were reported for both photoelectrochemical [6 – 11] and photovoltaic cells [12, 13] made of such materials. However, only crystals with smooth surfaces, prepared by careful cleavage, exhibited high quantum efficiencies, i.e. low recombination currents [6, 10, 14]. In a series of papers it was recently demonstrated that, using controlled anisotropic corrosion (CAC)*, one can produce highly photoactive WSe_2 "mixed" surfaces which contain both the $||c$ and $\perp c$ facets [15 – 18]. Fig. 1 shows an electron micrograph of a "mixed" surface of WSe_2. Such surfaces were shown to exhibit high quantum efficiency up to a wavelength of 1000 nm, and solar to electrical conversion efficiencies in excess of 12%, in polyiodide solution. This result was attributed to the favorable influence of the long diffusion length of minority carriers along the Van der Waals (VdW) plane [19] ($\perp c$) and fast charge transfer of carriers across the solid/electrolyte interface [17].

It is known that the WO_3, generated on the surface of WSe_2 during photocorrosion, can be dissolved using a solution of hot KOH [18, 20]. However, it was postulated [20] that a surface prepared by CAC contains a thin oxide film (2 to 4 monolayers = ML) on the $||c$ face, which is responsible for the recombination-free transfer of carriers across this face.

The structure and electronic properties of the electrochemically prepared WSe_2/WO_3 interface are not easy to understand because, associated with a change in the valency of the tungsten atom (from 4+ to 6+), substantial structural changes are involved. Moreover tungsten (and molybdenum) trioxides are known to have a number of polymorphic structures as well as non-stoichiometric compounds [21 – 23]. Furthermore a rich chemistry of tungsten bronzes

*) Mechanical indentation followed by photoelectrochemical etching and soaking in hot (60 °C) KOH, which dissolves the oxide film.

  0005-9021/93/0505-0702 $ 10.00+.25/0

Fig. 1
Typical electron micrograph image of a "mixed" WSe_2 surface prepared by mechanical indentation followed by photoetching and dissolution of the oxide by soaking in a hot KOH (CAC)

is documented [24], which emanates from the possibility to intercalate alkali ions and protons into the oxide lattice.

Being an indirect material [1], the cross section for radiative recombination in WSe_2 is low and consequently the luminescence intensity in this kind of material is extremely weak. However, if the "mixed" surface is exposed to a focused laser beam, a rather strong hot (i.e. above the bandgap) luminescence in the visible part of the spectrum is observed. Similar luminescence is obtained from $||c$ edges which are cut and allowed to slowly age in the air, but not from freshly exposed edges. The mechanism of this hot luminescence is discussed in some detail.

The present work deals with structural and optical properties of the WSe_2/tungsten-oxide interface. The photovoltaic results, which were published elsewhere [17], are discussed in view of the general semiconductor/oxide interface. Although the present model bears some similarity to the technologically important Si/SiO_2 interface, it is distinct from this interface in a number of important issues which are discussed below.

2. Experimental

n-Type WSe_2 (and also WS_2 and $MoSe_2$) crystals were grown by the chemical vapor transport technique with bromine as a transport agent [4]. Preparation of the semiconductor electrodes from WSe_2 crystals followed the procedures described in Refs. [15, 17]. Photoelectrochemical etching (PE), which produces the oxide film, was carried-out in an electrochemical set-up with a bias of +500 mV vs. Pt reference electrode, using 10% HCl solution. The color of the oxide film (<2000 Å thickness) was white, compared with the yellow color of thermally grown tungsten oxide. For the nuclear reaction analysis (NRA), PE was performed in 10% HCl solution containing 20% O^{18} (see Ref. [20]). A layer of a few hundreds Å of WO_3 was grown photoelectrochemically, assuming a density of 7.16 g cm^{-3} for the oxide [25]. The oxide layer was dissolved by soaking the electrode in 1 M KOH (60 °C) [19, 20]. NRA was carried-out, using 635 KeV resonance in the O^{18} (p, α)N^{15} reaction. The excitation source was a 2.4 MeV proton beam. The depth resolution of the technique was estimated at 50 Å. X-ray analysis (XRD) was performed with a powder diffractometer using CuK_α ($\lambda = 1.540598$ Å) radiation source, of energy 40 kV and a current of 100 mA. For the X-ray photoelectron spectroscopy (XPS) a small spot spectrometer with MgK_α radiation ($h\nu = 1253.6$ eV) was used. Photoluminescence (PL) measurements at different temperatures were carried out in a standard set-up equipped with double grating monochromator (Jobin Yvon HRD); liquid helium cryostat (TBT); Ar^+ ion laser (Coherent model Innova 90); and cooled photomultiplier (Hammamatsu RG942).

3. Results

3a. NRA. The purpose of these experiments were to find-out the thickness of the oxide layer after CAC. Table 1 summarizes the results of this experiment. The duration of the cleaning procedure was 5 min for the first soaking in KOH and another 5 min for the second soaking. Further soaking did not affect the count rate, and consequently it can be concluded that the thickness of the oxide layer, obtained after the second soaking (ca. 15 Å), is representative of the intimate oxide film chemisorbed onto the crystal surface, after CAC.

The thickness of the film was calculated using the following three hypotheses: 1. the oxide film is uniform, over the entire analyzed surface area; 2. the isotope ratio in the oxide (O^{16}/O^{18}) is similar to that in solution (4/1); 3. the oxidation of WSe_2 involves 14 holes according to the following reaction:

$$WSe_2 + 9H_2O + 14h^+ \rightarrow WO_3 + 2HSeO_3^- + 16H^+ \quad . \qquad (1)$$

Table 1 shows that the average thickness of the oxide layer after CAC (i.e. after KOH soak) has been completed, is about 1 – 2 ML. The quantum efficiency of photocorrosion processes has been found to exceed unity for many semiconductors in various electrolytes [26 – 28]. The larger than unity value of the quantum efficiency, in the present system, was attributed to the reaction of dissolved molecular oxygen with reaction intermediates at the electrode sur-

Table 1
Summary of the NRA analysis and calculated oxide thickness

mcoulomb/cm^2	counts PE	oxide thickness (Å)	counts 5 min KOH soak	oxide thickness (Å)	counts 10 min KOH soak	oxide thickness (Å)
750	37212	1785	656	31	224	11
300	14348	714	583	29	398	19
200	8763	480	438	24	175	10
200	4962	480	490	47	149	14

Table 2
Summary of the XRD data of tungsten oxide film grown by PE of WSe_2 and comparison with literature diffraction data

2 θ deg	calculated d (Å)	phase	literature		intensity
			d (Å)	(hkl)	
20	4.43	$W_{20}O_{58}$	4.28	(105)	1906
		$WO_{2.9}$	4.29	(105)	
34.2	2.62	$W_{20}O_{58}$	2.62	(116)	156
		$WO_{2.9}$	2.62	(116)	
37.3	2.40	$WO_{2.9}$	2.38	(217)	250
47.0	1.93	$W_{20}O_{58}$	1.96	(2011)	218
		$WO_{2.9}$	1.97	(2011)	
48.7	1.86	WO_3	1.86	(102)	187
		WO_3	1.86	(220)	
64.4	1.44	W_3O	1.45	(222)	218

face [20]. On the basis of our earlier work it can be concluded that, in the present experiments, the quantum efficiency, during CAC, may reach the values 1.2 – 1.5. Since the coverage of the surface by etch pits is not necessarily complete, a thicker oxide film is actually obtained on the covered parts. Thus an oxide layer of an estimated thickness of 2 – 4 ML is produced on WSe_2 after CAC.

3b. XRD: A few hundred angstrom thick oxide layer was prepared by PE and analyzed by XRD (see Table 2 and Fig. 2). Some distinct narrow crystalline peaks were superimposed on top of the X-ray spectrum of the WSe_2 lattice. Following this step the oxide layer was gradually dissolved by soaking the different samples in a hot KOH (60 °C) solution (1 M) for different periods of time. The X-ray spectrum of each sample was measured and analyzed. The strongest reflection peak of the partially dissolved oxide belonged to $WO_{2.9}$ ($W_{20}O_{58}$) and to a lesser extent to WO_3 and W_3O. After three minutes of dissolution time the W_3O was washed away and the remaining oxides were $WO_{2.9}$ and WO_3. The XRD spectrum of the oxides disappeared for (KOH) soaking times longer than 3 min, which suggested that the thickness of the remaining oxide film was below the detection limit of this technique.

It is likely that most of the thick oxide film consists of an amorphous phase, due to lattice relaxation. This is supported by electron diffraction measurements which were carried out on ca. 500 Å thick oxide film. However, a thin oxide film (< 50 Å) which is in intimate contact with the semiconductor is expected to preserve crystallinity and order.

3c. XPS: The interface between anodically grown oxide and WSe_2 has been studied in the past [29]. However, in the present study a very thin oxide film was prepared on the $\|c$ facet of the semiconductor, and consequently more detailed study of the intimate contact between the oxide and the semiconductor was possible. Samples for the XPS experiments were prepared in the following way. A cleaved WSe_2 sample was PE for ca. 20 min until etch pits as large as 200 μ were obtained. In this manner focusing of the XPS beam into a single etch pit became possible. Following careful soak in KOH and rinse, a pulse (< 1 s) PE was performed producing a thin oxide film of a calculated thickness of ca. 5 ML. Fig. 3 shows the XPS spectra of the W 4f line of the oxidized surface (0); after 1 ML of oxide

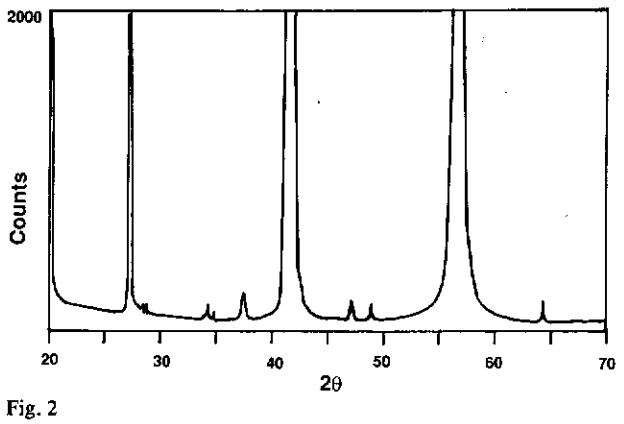

Fig. 2
XRD spectrum of tungsten oxides/WSe_2 interface prepared by PE. Oxide thickness is ca. 500 Å. Peaks at 27.5, 41.7 and 56.7° are obtained from reflections of the (004), (006), and (008) planes of WSe_2, respectively

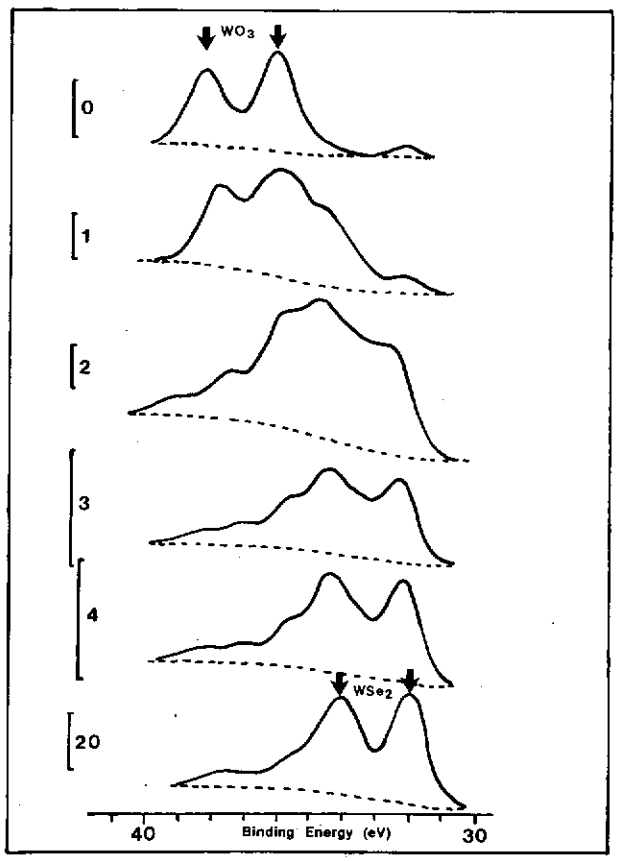

Fig. 3
XPS spectra of the 4f tungsten peak, taken from an interface of a composition 5 ML tungsten oxide/WSe_2. The bars on the left side represent 50 k counts; the number indicate the estimated number of oxide layers which were sputtered

was removed by argon sputtering (1), 2 ML of oxide sputtered (2), etc. The spectrum of the virgin surface is dominated by two lines of the tungsten oxide at 38.3 ($4f_{5/2}$) and 36.2 eV ($4f_{7/2}$), respectively. After sputtering of 4 ML the spectrum can be ascribed, mostly, to that of WSe_2 with two strong peaks at 34.1 and 32 eV. A rather surprising effect is the observation of an intermediate pair of peaks (37.5, 34.7 eV), which could be easily discerned after 2–4 ML sputtering.

Traces of tungsten oxide were present, even after 20 ML sputtering, suggesting that residual oxygen in the chamber (partial pressure of 10^{-9} torr) was preferentially adsorbed on the surface of the semiconductor. Dislocations, on the cleaved surface, and steps with exposed $||c$ facets, produced by CAC and subsequent sputtering, could serve as preferential sites for oxygen adsorption [30]. It is also remarkable that the XPS spectra of the same surface, but outside the etch pit, was very similar to that of a cleaved WSe_2 surface.

Similar shifts in the W 4f spectra were observed when 1 ML of oxide was grown on the WSe_2 by PE. However, in this case the change from W^{6+} (oxide) spectrum to that of W^{4+} (semiconductor) was much more abrupt, upon sputtering.

The oxygen 2 p spectrum was dominated by the 533.5 eV peak of a chemically bound oxygen. Physisorbed oxygen (531.2 eV) was predominant after sputtering of 4 ML. The source of the physisorbed oxygen could be either residual oxygen in the chamber or water molecules occluded in the electrochemically produced oxide. The Se 3 p line was absent on the virgin (oxide) surface and reappeared after 4 ML sputtering, although with lower intensity than expected.

3d. Luminescence: Since WSe_2 is an indirect semiconductor, radiative recombination from its lowest allowed transition is expected to be inefficient. It was noticed however that by focusing the laser beam onto the crystal edges ($||c$) or into the hexagonal etch pits, which are obtained through CAC, an intense luminescence emission is seen. Typical spectra obtained with WSe_2 crystal at 4.2 K are shown in Fig. 4. The two spectra, which are quite similar, correspond to the luminescence from a $||c$ edge (a) and from an etch pit (b). The spectra appear at higher energies than the fundamental bandgap of this material (approximately 1.2 eV at 300 K [31] and 1.3 eV at 4.2 K). Unlike sharp excitonic transitions the present spectra are rather broad. Very weak luminescence, only, was obtained from WSe_2 crystals which were PE and the oxide film (ca. 1000 Å) was left (by avoiding the final cleaning step with a solution of hot KOH) on their surface. This shows that the emission which is reported here can not be ascribed to the electrochemically grown WO_3 film. Polarization experiments were performed, i.e., the light was polarized in different directions with respect to the sample. These experiments did not produce any conclusive data. In contrast with the atomically smooth VdW plan ($\perp c$) the surface, from which emission is obtained is highly textured, and the orientation of the wavevector of the polarized beam with respect to the two components of the original surface ($\perp c$ and $||c$) is not well defined in this case.

Cathodoluminescence (CL) experiments at low temperatures (down to 4.2 K) showed that the emission was obtained from the entire $||c$ edge, however intense emission is associated with "hot" spots on the $||c$ edge. The spectral distribution of the CL was found to be very similar to that of the PL. Fig. 5 shows that the emission is confined to the $||c$ edge of a crystal (which was CAC treated), only. No CL was obtained from the VdW face of the crystal. The excitation source in this case is an electron beam having an energy of a few keV. The fact that both PL and CL occur from the same (lowest) radiative state, suggest that the luminescence occurs from a fundamental lowest transition and thus the PL can not be ascribed to an intermediate state which exists in the middle of the bandgap (e.g. from an oxide). Fig. 6 shows a comparison of the PL spectra of WSe_2, WS_2, and $MoSe_2$. The two former crystals were left for a few weeks in the ambient atmosphere of the laboratory and the luminescence was obtained from essentially the entire surface of

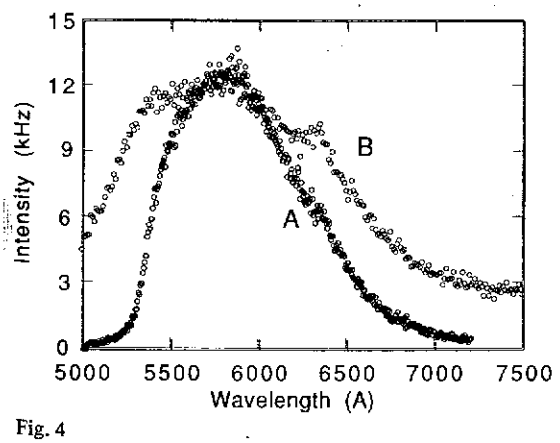

Fig. 4
Typical photoluminescence spectra obtained on the $||c$ facets of a WSe_2 crystal at 4.2 K. a. $||c$ edge; b. from an etch pit

Fig. 5
Secondary electron (left) and cathodoluminescence (right) images of the boundary zone of VdW ($\perp c$)-top; and $||c$ edge-down, of a WSe_2 crystal at 100 K. Bar is 100 µm. Note that no CL is obtained from the VdW ($\perp c$) face of the crystal

the $||c$ edges. Contrarily in $MoSe_2$ crystal was taken from the evacuated ampoule, put into the cryostat where it was preserved under inert atmosphere during cool-down period, and measured one day later. The luminescence of the $MoSe_2$ crystal occurred from a single spot on the $||c$ edge. The luminescing hot spot was the result of either a very fast aging, or from an impurity (e.g. bromine form the chemical vapor transport). To further illustrate the influence of aging time, the edges of WSe_2 crystals which gave very intense luminescence were cut with a blade and introduced into the cryostat immediately after that and maintained under inert atmosphere during cool down. A very weak luminescence was observed in this case, which shows that the luminescence is obtained only after aging in ambient conditions or within an etch pit obtained by CAC. The temperature dependence of the (peak) luminescence intensity $I(T)$ in WSe_2 was determined. Fig. 7 shows a plot of $\ln(I(T)/I(4.2\,\mathrm{K})-1)$

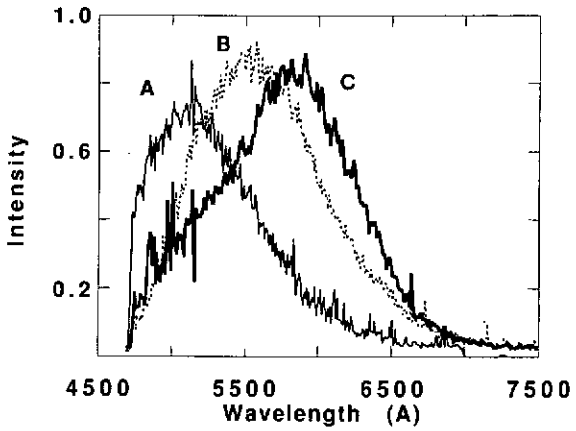

Fig. 6
Comparison of the PL obtained from the $||c$ edges of three crystals: A) $MoSe_2$; B) WS_2; and C) WSe_2

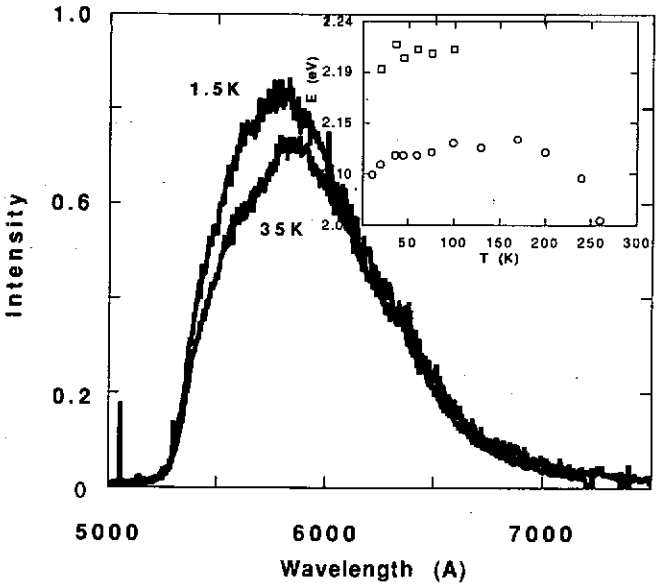

Fig. 7
Activation energy for the dissociation of the luminescing center (84 meV) obtained from the slope of $\ln(I(T)/I(4.2\,\mathrm{K})-1)$ vs. $1/T$ (temperature dependence of the luminescence intensity)

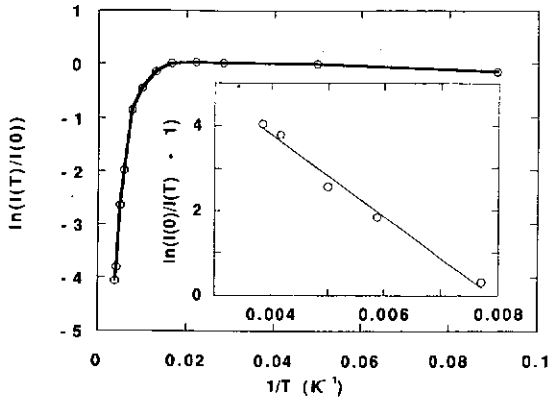

Fig. 8
Variation of the PL lineshape on temperature. Inset presents the dependence of the peak and shoulder energies on temperature

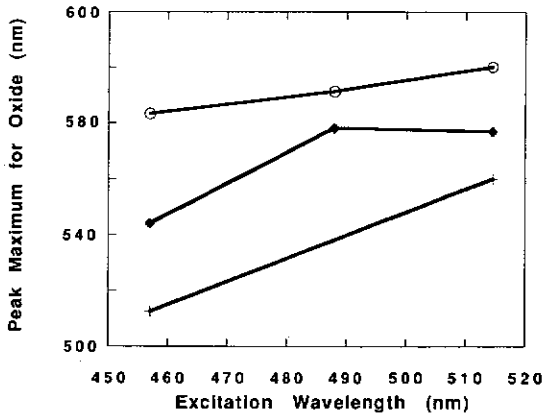

Fig. 9
Dependence of the peak position and the FWHM of the peak on the excitation wavelength: (◆) $MoSe_2$; (+) WS_2; (⊙) WSe_2

vs. $1/T$. From the slope of this curve an activation barrier for the dissociation of the luminescing center was calculated (84 meV). The lineshape of the emission changed with temperature. At low temperatures the emission consisted usually of a broad single peak which position did not change with temperature. At temperatures of 35 K and higher a distinct new shoulder at energy larger than the original peak was observed and the spectrum exhibited a red shift. Fig. 8 shows the PL spectra at 1.5 and 35 K, and the changes in the peak and shoulder position with temperature (inset). The intensity of the luminescence was found to increase linearly with the excitation light intensity over two orders of magnitude (1 – 200 mW). The emission peak exhibited a blue shift with decreasing excitation wavelength as shown in Fig. 9. The full width at half maximum (FWHM) decreased with an increase in the excitation wavelength as shown also in Fig. 9.

4. Discussion

The main conclusions of the present study are the following:

1. A thin oxide film of 2–4 ML is left on the $||c$ edges (facets) of WSe_2 after CAC.

2. This oxide film is crystalline and consists mostly WO_3 related phases.
3. The structure and valency of W atoms undergo substantial changes across this interface. In the semiconductor side W^{4+} with tetrahedral bonding exists, while W^{6+} with octahedral structure is predominant on the oxide side.
4. Strong hot luminescence is observed by excitation of a CAC-treated surface and the $||c$ edges of a crystal which was allowed to "age" for a few weeks in ambient conditions.

A remarkable property of the initially sputtered surface (Sect. 3c) is the observation of an intermediate state of the W 4f peak (37.5, 34.7 eV). This intermediate state essentially disappeared after sputtering of 4 ML of oxide and was totally absent after sputtering of 20 ML of material. Tungsten is not a stable moiety, in general, in the 5+ valency [32]. Nevertheless a stable W^{5+} state exists in tungsten bronzes of the form MWO_3 [24]. Furthermore the coloration of amorphous WO_3, upon electrochemical reduction, was attributed to the stabilization of the W^{5+} state due to potential fluctuations in the disordered film [33]. It would be tempting to suggest that the intermediate state, observed by XPS, is W^{5+} stabilized by the interface between the oxide (W^{6+}), and the WSe_2 (W^{4+}). However, it is well known that ion-bombarded WO_3 films tend to loose oxygen with the consequence that a non-stoichiometric intermediate with valency $<6+$ appears in the spectrum [34]. Ideally one would like to probe such intermediate state, at the WSe_2/WO_3 interface nondestructively, e.g. by tilting the sample relative to the probe beam of the XPS. However, this technique is not easy to apply in the present case where a focused beam is probing the $||c$ facets of a deep etch pit. In conclusion, although some indications for the existence of an intermediate tungsten 5+ exist, at the semiconductor/oxide interface, more careful analysis is necessary to prove its exact nature.

Band structure calculations [35] show that the valence band of WSe_2 consists mainly of W 5 d_{z^2} and Se 3 p_z orbitals. The main contributions to the conduction band come from W 5 d_{xy}, 5 $d_{x^2-y^2}$, Se 3 p_x and 3 p_y. Thus the orbitals of the valence band are concentrated along the $||c$ (z) direction, while the orbitals of the conduction band are directed towards the $\perp c$ (x,y) axis. It can be expected, therefore, that the dangling bonds, on the ($||c$) steps of the etch pits, are associated with unsaturated orbitals (W 5 d_{xy}, 5 $d_{x^2-y^2}$ and perhaps Se 3 p_x and 3 p_y) derived from the conduction band. It can also be concluded that these states, which serve as recombination centers, are located within the forbidden gap and close to the conduction band of WSe_2, as suggested earlier [36]. Since these states are located near the conduction band and below the Fermi level, they can be regarded as donor states which are occupied by conduction band electrons. Such states behave like ideal recombination centers for valence band holes which are drifted to the semiconductor surface. The effect of oxygen anneal or wet (electro)chemical oxidation on similar states in Cd-chalcogenide and ternary chalcopyrite semiconductors has been discussed in detail by Cahen and Noufi [37]. It was suggested that the oxygen binds to the metal atom thereby leading to a decrease in the free carrier (electron) density of the semiconductor by saturating the dangling bonds of the metal atoms or passivating the charge of the chalcogen vacancy at the surface. Note however that the above model is pertinent to p-type semiconductors, whereas here an n-type semiconductor/oxide interface is considered.

The crystal structure of WO_3 resembles that of a simple cubic ReO_3 structure [32]. Each Re atom is octahedrically coordinated to 6 oxygen atoms. These octahedra are linked by their corners so that each oxygen is shared by two octahedra of Re atoms. Each octahedra is thus a ReO_3 unit. The structure of WO_3 is slightly distorted, however, so that its symmetry is monoclinic of type MX_6 [32]. This type of structure exhibits sp^3d^2 hybridization.

In view of the preferred octahedral arrangement of WO_3 molecules it is proposed that distorted octahedra exist on the $||c$ surface of the CAC treated WSe_2. The oxygen atoms at the $||c$ edges, glue (zip) the separate WSe_2 atomic layers, which were originally held together by VdW forces. This zipped structure provides the missing 2 p electrons for the vicinal W atoms, and satisfies the conditions for the sp^3d^2 hybridization of the oxide. It further promotes the mechanical stability of the interface, and averts the intercalation of alkali ions and protons into the lattice, an effect which could adversely affect the photovoltaic response of the material. Therefore the crystalline oxide layer provides the conditions for saturation of the dangling bonds, prohibiting thus surface states, associated with W 5 d_{xy}, 5 $d_{x^2-y^2}$ orbitals, which are responsible for surface recombination and loss of quantum efficiency.

Since the flatband potential of WO_3 (0 to 0.3 eV vs. NHE [38]) is similar to that of WSe_2 [39], it is not likely to provide the electric field necessary to drive space charge electrons away from the surface, which reduces surface recombination, as is the case for Si/SiO_2 interface [40, 41]. Indeed CAC does not lead to reduction of majority carriers (dark) current, as observed for the Si/SiO_2 interface, and consequently no gain in the open circuit potential is expected in this case. Also, most of the difference in the bandgap of the two compounds (ca. 1.5 eV) is associated with the discontinuity in the valence band of the two semiconductors. Therefore effective tunneling of the holes across the oxide layer is possible only for very thin ($<40-50$ Å) oxides. Although this picture is schematic and tentative, it provides the framework for the understanding of the effect of CAC in layered semiconductors, and a working hypothesis for continuation of this research.

The next step will be to study in detail the electronic structure of this interface and its evolution in polyiodide solution under operational conditions of the photoelectrochemical cell. This study may enable us to explain the high conversion efficiencies reported for such photoelectrochemical cells, recently [15, 17].

The energy bandgap of tungsten oxide is ca. 2.8 eV (460 nm) at 4.2 K. Excitation of the sample with 457, 488 and 514 nm light did not affect the PL lineshape remarkably, apart from a small shift in the peak (see Fig. 9). Ex-

citation of the material with a few keV electron beam led to a CL spectrum with a maximum at 570 nm which is very similar to the PL spectrum. The emission energy is appreciably smaller than the bandgap of the oxide. These facts suggest that the thin tungsten oxide film is not responsible for the observed PL. The luminescence peak of MoO_3 was found to be 440 nm [42], far below the wavelength of the presently reported emission. Since the oxide film found after CAC is 10 – 20 Å thick, it is not expected to absorb efficiently the light, and remit. It can be concluded therefore that the luminescence can not be ascribed to the pure oxide.

Electrochemical intercalation of hydrogen and alkali metals, in tungsten and molybdenum oxides, under cathodic bias, was shown to lead to substantial shifts of the absorption edge of the original oxides into the visible range of the spectrum [33, 43, 44]). Since the CAC is performed under anodic conditions, where intercalation of such atoms is unlikely, the observed luminescence can not be explained by hydrogen and alkali metals intercalation (note however that hydrogen intercalation is found in Si anodized in HF solution, which is one of the proposed mechanisms for the luminescence of porous silicon [45]).

The indirect bandgap of all three materials is similar (1.3 eV). However the direct gap of WS_2 (1.85 – 1.9 eV) is larger than that of WSe_2 (1.45 eV) [30] (generally the bandgap at 4.2 K is about 0.1 eV larger than at 300 K). As for $MoSe_2$ its direct gap is similar to that of WSe_2. The fact that the luminescence appears on the edges and within etch pits of the CAC treated surface suggested to us that the selection rules might be different for excitation along the two main axis ($\perp c$ and $||c$). However, the fact that a freshly cut surface did not show any luminescence did not support this mechanism.

The large activation energy of the luminescing center (84 meV) excludes a simple excitonic mechanism. This conclusion is further supported by the large FWHM of the emission.

PL through Auger recombination at energies which are appreciably larger than the energy gap, were reported recently [46]. However such emission is not expected to be limited to the $||c$ edges and is likely to be very weak. Therefore this mechanism can be excluded as a possible explanation for the present results.

Two plausible mechanisms for the observed emission are 1. quantum confinement of excitons at the $||c$ edges and 2. luminescence from a mixed oxide formed at the $||c$ edges by either aging or CAC.

1. At the $||c$ edges of the crystal a gap may be opened at random between two WSe_2 layers every few atomic layers, by intercalation of an oxide. Such a gap may be induced by already present impurity, which weakens the VdW forces binding the layers together. This gap may be formed during CAC or through simple aging of the crystal. The gap between the layers will induce strong localization of excitons at the $||c$ edges, and hence will enhance the emission of light. The present measurements indicate that the penetration depth of the oxide is very shallow and hence the gap between the layers will close on itself toward the bulk of the material, which explains two facts: a. the luminescence is observed at $||c$ edges of the crystal, only, and b. light which is incident on the $||c$ edges and penetrates deeper into the material leads to a red shift in the luminescence spectrum because the gaps gradually coalesce toward the bulk and hence the quantum confinement is weaker. Although more measurements are necessary to ascertain this model, this model casts a fresh view on quantum confinement of carriers in anodically formed structures. Similar model was offered recently to explain the room temperature luminescence of porous silicon which is formed by anodization in HF solution [47].

2. The possibility of formation of a mixed tungsten-sulfur oxide, which is responsible for the observed luminescence, can not be excluded. Both XPS and NRA measurements suggest that a thin oxide is formed on the $||C$ edges as a result of CAC. The verification of the chemical nature of the oxide is very difficult, and is beyond the scope of this work.

Further work is necessary to distinguish between the two models.

We are indebted to Dr. Lev Margulis of the Weizmann Institute for his assistance with the XRD measurements, and for the staff of the Accelerators Center of the Weizmann Institute for their assistance with the NRA analysis. We also thank the Isotope Separation Unit of the Weizmann Institute for donation of the H_2O^{18}, used for the NRA experiments. We are grateful to Dr. R. Brener of the Technion, Haifa, for his suggestions regarding the XPS results. This work was supported in part by a grant from the National Council for Research and Development, Israel, and the KFA, Jülich, FRG. D.H.W. acknowledges support from the Department of Energy of the USA.

References

[1] J.A. Wilson and A.D. Yoffe, Adv. Phys. *18*, 193 (1969).
[2] W.Y. Liang, J. Phys. C. *6*, 551 (1973).
[3] A.R. Beal, Y.Y. Liang, and H.P. Hughes, J. Phys. C. *9*, 2449 (1976).
[4] L.C. Upadhyayula, J.J. Laferski, A. Wold, W. Giriat, and R. Kershew, J. Appl. Phys. *39*, 4736 (1968).
[5] H. Tributsch, Ber. Bunsenges. Phys. Chem. *81*, 361 (1977); Structure and Bonding, *49*, 127, Springer Verlag, Berlin 1982.
[6] B. Parkinson, Acc. Chem. Res. *17*, 431 (1984).
[7] H.J. Lewerenz, A. Heller, F.J. Di-Salvo, J. Anal. Chem. Soc. *102*, 1877 (1980).
[8] F.R. Fan, H.S. White, B. Wheeler, and A.J. Bard, J. Electrochem Soc. *127*, 519 (1980).
[9] C.P. Kubiak, L.F. Schneemeyer, and M.S. Wrighton, J. Am. Chem. Soc. *102*, 6898 (1980).
[10] L. De-Angelis, E. Scafe, F. Galluzzi, L. Fornarini, and B. Scrosati, J. Electrochem. Soc. *129*, 1237 (1982).
[11] C.A. Koval and J.B. Olson, J. Electroanal. Chem. *234*, 133 (1988).
[12] a. M. Vögt, M. Lux-Steiner, H.-P. Schweikardt, P. Dolatzoglou, M. Keil, W. Reetz, and E. Bucher, Proc. 4th Intl. Natl. PVSEC, IREE *493* (1989); b. E. Bucher, Statusreport 1990, Photovoltaics, *33*, 1, Ed. R. Urban, BEO, Forschungszentrum Jülich 1990.
[13] M. Vögt, M. Lux-Steiner, P. Dolatzoglou, and E. Bucher, Proc. 8th E.C. Photovoltaic Solar Energy Conf. 1112, Kluwer Acad. Publ. Dordrecht, Boston 1988.
[14] H.J. Lewerenz, A. Heller, and F.J. DiSalvo, J. Am. Chem. Soc. *102*, 1877 (1980).

[15] a. R. Tenne and A. Wold, Appl. Phys. Lett. *47*, 707 (1985); b. D. Mahalu, A. Jakubowicz, A. Wold, and R. Tenne, Phys. Rev. B. *38*, 1533 (1988); c. A. Jakubowicz, D. Mahalu, M. Wolf, A. Wold, and R. Tenne, Phys. Rev. B *40*, 2992 (1989).
[16] O.N. Srivastava and G. Prasad, J. Phys. D *21*, 1028 (1988).
[17] D. Mahalu, L. Margulis, A. Wold, and R. Tenne, Phys. Rev. B, Rapid Commun. *45*, 1943 (1992).
[18] V. Nabutovsky, K. Eherman, and R. Tenne, submitted.
[19] W. Kautek and H. Gerischer, Surf. Sci. *119*, 46 (1982).
[20] D. Mahalu, M. Peisach, W. Jaegerman, A. Wold, and R. Tenne, J. Phys. Chem. *94*, 8012 (1990).
[21] S.K. Deb, J. Appl. Phys. *37*, 4818 (1966); Philos. Mag. *27*, 801 (1973).
[22] T.H. Fleisch and G.J. Mains, J. Chem. Phys. *76*, 780 (1982).
[23] J.N. Yao, K. Hashimoto, and A. Fujishima, Nature *355*, 624 (1992).
[24] Chemistry of the Elements, p. 1185, N.N. Greenwood and A. Earnshaw, Pergamon Press, Oxford 1990.
[25] Handbook of Chemistry and Physics, 69th edition, p. B-141, ed. R.C. Weast, CRC Press Inc., Florida 1988.
[26] a. M. Matsumura and S.R. Morrison, J. Electroanal. Chem. *147*, 157 (1983); b. H.J. Lewerenz, J. Stumper, and L.M. Peter, Phys. Rev. Lett. *61*, 1989 (1988).
[27] a. W.H. Brattain and C.G. Garret, Bell. Syst. Tech. J. *34*, 129 (1955); b. H. Gerischer and F. Beck, Z. Phys. Chem. Neue Folge *24*, 378 (1960).
[28] V. Marcu, R. Tenne, and I. Rubinstein, J. Electrochem. Soc. *133*, 1143 (1986).
[29] a. W. Jaegermann, in Photoelectrochemistry and Photovoltaics of Layered Semiconductors, pp. 246–249. Ed. A. Aruchamy, Kluwer Academic Publishers, Dordrecht 1992; b. W. Jaegermann and D. Schmeisser, Surf. Sci. *165*, 143 (1986).
[30] Z. Shuxian, W.K. Hall, G. Ertel, and H. Knözinger, J. Catal. *100*, 167 (1986).
[31] K.K. Kam and B.A. Parkinson, J. Phys. Chem. *86*, 463 (1982).
[32] a. E. Cartmell and G.W.A. Fowles, Valency and Molecular Structure, 2nd Edn (1961); b. A. Cotton and G. Wilkinson
[33] O.F. Schirmer, V. Wittwer, G. Baur, and G. Brandt, J. Electrochem. Soc. *124*, 749 (1977).
[34] a. R. Holm and S. Storp, Appl. Phys. *12*, 101 (1977); b. T.J. Driscoll, L.D. McCormick, and W.C. Lederer, Surf. Sci. *187*, 539 (1987).
[35] R. Coehoorn, C. Haas, and R.A. de Groot, Phys. Rev. B *35*, 6203 (1987).
[36] a. S.M. Ahmed and H. Gerischer, Electrochim. Acta *24*, 705 (1979); b. B.A. Parkinson, T.E. Furtak, D. Canfield, K.K. Kam, and G. Kline, Faraday Discuss. *70*, 1 (1980).
[37] D. Cahen and R. Noufi, Appl. Phys. Lett. *54*, 558 (1989); Solar Cells *30*, 53 (1991).
[38] a. M.A. Butler, J. Appl. Phys. *48*, 1914 (1977); b. W. Gissler and R. Memming, J. Electrochem. Soc. *124*, 1710 (1977).
[39] A.J. McEvoy, M. Etman, and R. Memming, J. Electroanal. Chem. *190*, 225 (1985).
[40] S.M. Sze, Physics of Semiconductor Devices, 2nd edition.
[41] P. van Halen, R.P. Merlens, R.J. Overstraeten, R.E. Thomas, and J. van Meerbergen, IEEE Trans. Electron. Devices *25*, 507 (1978).
[42] M. Anpo, T. Suzuki, Y. Kubokawa, F. Tanaka, and S. Yamashita, J. Phys. Chem. *88*, 5778 (1984).
[43] a. H.O. da Frota, H. Panepucci, A. Cruz-Orea, E.A. Romero Coss, P.M. Raccah, F. Sanchez-Sinencio, and J.S. Helman, Solid State Commun. *49*, 921 (1984); b. Y. Hiruta, M. Kitao, and S. Yamada, Jpn. J. Appl. Phys. *23*, 1624 (1984).
[44] J.F. Owen, K.J. Teegarden, and H.R. Shanks, Phys. Rev. B *18*, 3827 (1978).
[45] S.M. Prokes, O.J. Glembocki, V.M. Bermudez, R. Kaplan, L.E. Friedersdorf, and P.C. Searson, Phys. Rev. B, Rapid Commun. *45*, 13788 (1992).
[46] A. Hangleiter, Phys. Rev. Lett. *55*, 2976 (1985).
[47] L.T. Canham, Appl. Phys. Lett. *57*, 1046 (1990).

(Received: August 25, 1992; E 8135
final version: February 11, 1993)

In Situ High Temperature SERS Study of Oxygen Adsorbed on Ag: Support and Electrochemical Promotion Effects

D.I. Kondarides, G.N. Papatheodorou, C.G. Vayenas, and X.E. Verykios

Institute of Chemical Engineering and High Temperature Chemical Processes and Department of Chemical Engineering, University of Patras, P.O.Box 1414, GR-26500, Patras, Greece

Key Words: Adsorption / Catalysis / Electrochemistry / Spectroscopy, Raman

In situ surface enhanced Raman spectra (SERS) of adsorbed oxygen were obtained during oxygen adsorption and ethylene epoxidation on Ag catalyst surfaces at temperatures between 25 and 400 °C and atmospheric total pressure. Three types of Ag catalysts were investigated: (I) Ag supported on α-Al_2O_3, (II) Ag films deposited on quartz and (III) Ag films deposited on the O^{2-} conducting solid electrolyte Y_2O_3-stabilized ZrO_2 (YSZ). In the last case the effect of the application of external voltages (−2 V to +2 V) on the SERS was also examined "in situ" in order to investigate the effect of Non-Faradaic Electrochemical Modification of Catalytic Activity (NEMCA). Bands at 240, 345, 815, 870, 980 and 1630 cm^{-1} were observed for the oxygen-Ag/YSZ system. The 815 and 980 cm^{-1} bands were also observed for the Ag/quartz and Ag/α-Al_2O_3 samples. The intense band at 815 cm^{-1}, assigned to the O–O stretching vibration of a molecularly adsorbed oxygen species, exhibited an isotope shift of 20 cm^{-1} upon replacing $^{16}O_2$ with $^{18}O_2$. This band is present during ethylene epoxidation at temperatures up to 350 °C and its relative Raman intensity decreases with decreasing O_2 to C_2H_4 ratio. The excitation profile of the 815 cm^{-1} band and the existence of the overtone at 1630 cm^{-1} indicate that preresonance Raman enhancement is also responsible for the high intensity spectra obtained. In the case of Ag/YSZ it was found that increasing catalyst potential strengthens the O–O bond and increases the band intensity, while decreasing catalyst potential causes a decrease in bond strength and band intensity. These observations can be accounted for within the framework of previous NEMCA studies. However the change in relative band intensity can also be due to the effect of applied voltage and changing Fermi level and work function on the enhancing mechanism of SERS.

  0005-9021/93/0505-0709 $ 10.00+.25/0